

FRACTURE CRITERION ANALYSIS AND CRACK GROWTH PROPERTY OF MIXED-MODE CRACK EXPERIMENTS

SU Shaopu¹, ZHANG Wendong¹, LI Lei¹

¹Aircraft Strength Research Institute, Xi'an, China

Abstract

The fracture criterion and crack growth behavior of Compact Tension Shear (CTS) specimens are studied under different loading modes in this paper. Crack deflection angles, the limit loads of mixed-mode structure, the apparent fracture toughness and the crack growth model have been obtained both experimentally and numerically. The research investigates that, the crack of CTS specimen extends vertically along the loading direction, and Tanaka formula is adequate to represent the equivalent stress intensity factor for CTS specimens. Maximum circumferential normal stress (MTS) criterion and Richard criterion can obtain the conservative evaluation compared with experiments. Based on experimental results, a formula for fracture evaluation and a new model for mixed-mode crack growth prediction are proposed to evaluate the damage tolerance property of mixed-mode crack structure.

Keywords: Mixed-mode fracture criterion; Mixed mode I-II; Compact Tension Shear specimen; Crack growth model

1. Introduction

With the development of advanced manufacturing technology on aircraft, integral structure becomes more and more popular in the engineering design owing to its characters of lightweight and high safety. The new type of aircraft structure may be in the combination of tensile, bending or shear stress state. Consequently, the damage tolerance studies of structures under mixed-mode loading play an imperative role in its structural integrity assessment.

Based on the standard Compact Tension Shear (CTS) specimen, the fracture criterion and crack growth behavior of mixed-mode crack experiments are analyzed by experiments and Finite Element (FE) model in this paper. The relation between residual strength and loading angle are presented based on experimental results, and a new fracture criterion is proposed to evaluate the loading ability of CTS specimens. Considering that the relation between mode-I /II stress intensity factors (SIF) and crack growth step are the key points to predict the fatigue life of mixed-mode crack experiments, we validate the feasibility of different forms of equivalent SIF on the estimation of crack growth life, and the results show that Tanaka formula is more adequate to calculate the equivalent stress intensity factor for CTS specimens among 4 forms of equivalent SIF. In addition, a crack growth model based on K_I and K_{II} is discussed to evaluate the crack growth life of mixed-mode crack tests.

2. Theories for 2D Mixed-mode Fracture Mechanics

2.1 Mixed-mode Fracture Criterion

Erdogan and Sih [1] proposed a maximum circumferential normal stress (MTS) criterion to analyze a structure with mixed-mode crack. For a two dimensional crack in an infinite plate, the Airy stress function can be used to describe the complete stress of cracked structure, and the crack deflection angle θ^* can be deduced as:

$$K_I \sin \theta^* + K_{II} (3 \cos \theta^* - 1) = 0 \quad (1)$$

where K_I and K_{II} are respectively the mode-I and mode-II SIF. For mode I-II crack structure, the critical fracture condition is:

$$1 = \cos \frac{\theta}{2} \left[\frac{K_I}{K_{IC}} \cos^2 \frac{\theta}{2} - \frac{3}{2} \frac{K_{II}}{K_{IC}} \sin \theta \right] \quad (2)$$

Where K_{IC} is mode-I fracture toughness, its unit is $\text{MPa}\sqrt{\text{mm}}$. As the assumption of linear elasticity state, the fracture formula obtained by maximum energy release rate is the same as the one by MTS criteria.

2.2 Minimum Strain Energy Density Criterion (SED)

The strain energy density factor of crack tip in 2D, defined as S , is written as [2]:

$$S = a_{11}k_I^2 + 2a_{12}k_Ik_{II} + a_{22}k_{II}^2 \quad (3)$$

where k_I is effective SIF in mode-I state, $k_I = K_I / \sqrt{\pi}$, its unit is $\text{MPa}\sqrt{\text{mm}}$; k_{II} is effective SIF in Mode-II state, $k_{II} = K_{II} / \sqrt{\pi}$, its unit is $\text{MPa}\sqrt{\text{mm}}$. The coefficients a_{11} , a_{12} and a_{22} are related to the values of polar angle θ , elastic modulus E and Poisson's ratio ν :

$$\begin{cases} 16\mu a_{11} = (1 + \cos \theta)(\kappa - \cos \theta) \\ 16\mu a_{12} = \sin \theta [2 \cos \theta - (\kappa - 1)] \\ 16\mu a_{22} = (\kappa + 1)(1 - \cos \theta) + (1 + \cos \theta)(3 \cos \theta - 1) \end{cases} \quad (4)$$

The crack is assumed to grow along the direction where S reaches to the minimum value of the sphere surface, the crack deflection angle is determined when:

$$\left[\frac{\partial S}{\partial \theta} \right]_{\theta^*} = 0, \left[\frac{\partial^2 S}{\partial \theta^2} \right]_{\theta^*} > 0 \quad (5)$$

Sih proposed that the critical strain energy S_{cr} is defined as:

$$S_{cr} = \frac{1}{8\mu} (\kappa - 1) k_{IC}^2 \quad (6)$$

Where K_{IC} is Mode-I fracture roughness, and $k_{IC} = K_{IC} / \sqrt{\pi}$, its unit is $\text{MPa}\sqrt{\text{mm}}$. The structure will fail if S_{min} reaches to S_{cr} , the critical load can be derived from formula (6).

2.3 Von Mises Fracture Criterion (VMF)

This criterion is built based on the following assumption [3]:

- The crack always propagates along the shortest path through the plastic zone to the elastic zone, and the formed angle is defined as initial deflection angle;
- When the elastic-plastic boundary polar radius is larger than the critical radius r_c , crack begins to propagate.

The elastic-plastic boundary polar radius is written as:

$$r(\theta, K_I, K_{II}) = \frac{1}{8\pi C} [c_{11}K_I^2 + 2c_{12}K_IK_{II} + c_{22}K_{II}^2] \quad (7)$$

Where

$$\begin{aligned} c_{11} &= \xi(1 + \cos \theta) + \sin^2 \theta \\ c_{12} &= \sin(2\theta) - \xi \sin \theta \\ c_{22} &= 1 + \xi(1 - \cos \theta) + 3 \cos^2 \theta \\ \xi &= \frac{2(1 - 2\nu^*)^2}{3} \end{aligned} \quad (8)$$

Here $\nu^* = 0$ for plane stress problem; $\nu^* = \nu$ for plane strain.

Assumed that the critical polar radius of mixed-mode crack is constant, and it can be calibrated by the critical polar radius of mode-I or mode-II cracked structure, r_{cr} can be written as following:

For mode-I crack:

$$r_{cr} = \frac{\xi K_{IC}^2}{4\pi C} \quad (9)$$

Where r_{cr} is the critical radius of model-I crack, its unit is mm.

For model-II crack:

$$r_{cII} = \frac{K_{IC}^2}{8\pi C} \left(1 + \xi - \frac{\xi^2}{12} \right) \quad (10)$$

Where r_{cII} is the critical radius of model-II crack, its unit is mm.

If r_{cI} is a known material parameter, the critical fracture formula is written as following:

$$c_{11}K_I^2 + 2c_{12}K_IK_{II} + c_{22}K_{II}^2 = 2\xi K_{IC}^2 \quad (11)$$

2.4 Fracture criterion by Richard

A comparative stress intensity factor K_V is proposed by Richard [4], which depends on the stress intensity factor K_I and K_{II} :

$$K_V = \frac{K_I}{2} + \frac{1}{2} \sqrt{K_I^2 + 4(\alpha_1 K_{II})^2} \quad (12)$$

Where the material parameter α_1 describes the ratio of fracture toughness for model-I and model-II cracks, $\alpha_1 = \frac{K_{IC}}{K_{IIC}}$. α_1 is set to 1.155 in reference [4] for isotropic material.

Unstable crack growth occurs as soon as K_V is greater than K_{IC} , which is written as:

$$K_V = K_{IC} \quad (13)$$

Based on a large number of experiments, Richard obtained that the crack deflection angle satisfies the following relation:

$$\theta^* = \mp \left[155.5^\circ \frac{|K_{II}|}{|K_I| + |K_{II}|} \right] - 83.4^\circ \left[\frac{|K_{II}|}{|K_I| + |K_{II}|} \right] \quad (14)$$

Where $\theta^* < 0$ when $K_{II} > 0$ and vice versa, which is described in Figure 1.

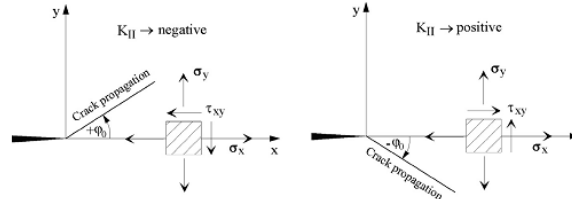


Figure 1 – Crack deflection angle of structure under mixed-mode loading [4]

2.5 Fatigue Crack Growth Model in Mixed-mode State

The fracture mechanics parameters, such as strain energy release rate, the mode-I and mode-II SIF and J-integral, were applied to represent crack propagation rate in mixed-mode models. Here we apply Paris type equation to analyze the fatigue crack growth rate. Due to the interference between multiple cracks, the crack tip may be in the mixed-mode stress state. So we express the fatigue crack growth rate as a function of the equivalent SIF K_{eff} as following:

$$\frac{da}{dN} = c (\Delta K_{eff})^n \quad (15)$$

Where c, n are material parameters, ΔK_{eff} is the amplitude of K_{eff} under maximum loading and minimum loading.

The key point is that how to describe the equivalent factor in the form of mode-I, mode-II and mode-III SIF (noted as K_I , K_{II} and K_{III}). Some work has been done in this research field. Yan proposed the following MTS formula [5] to describe K_{eff} :

$$K_{eq} = K_I \cos^3 \frac{\theta}{2} - 3K_{II} \cos^2 \frac{\theta}{2} \sin \frac{\theta}{2} \quad (16)$$

Where θ is the crack growth direction.

Tanaka proposed a corrected K_{eff} based on the experimental results [6], as shown in following:

$$K_{eq} = [K_I^4 + 8K_{II}^4]^{0.25} \quad (17)$$

In addition, Tanaka suggests that this criterion can be extended to analyze the crack problem under three mode loadings.

Meanwhile, most commercial software applies the simple square root formula to consider the coupling effect of K_I and K_{II} as following:

$$K_{eq} = \sqrt{K_I^2 + K_{II}^2 + (1-\nu)K_{III}^2} \quad (18)$$

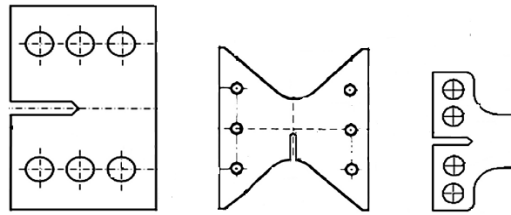
Where ν is the passion ratio.

3. Experimental Investigations of Mixed-mode CTS Specimen

The thickness of specimens studied in this paper is 5mm, which is a plane stress problem. Because there is no experimental standard to follow for mixed-mode crack experiments, we cannot obtain the relation between the crack length and the crack opening width. Therefore we apply the apparent fracture toughness K_{app} to evaluate the structural residual strength. K_{app} is the value of SIF for the structure with initial crack length on failure load, which can be used as the ultimate residual strength when the tear material suddenly fractures.

3.1 CTS Specimen and Loading Form

Different types of specimens have been designed to study the mixed-mode crack, as shown in Figure 2. CTS specimen, recognized as the most common specimen form, was proposed by Richard in the eighties of last century [7], Zhao et al [8] designed a small version of CTS structure to analyze the mode I-II crack; Fig. 2b) is the butterfly-type specimen proposed by Arcan [9]; In order to reduce the usability of materials, Demir [10] proposed a T-shaped specimen and verified its feasibility through the experiments. In consideration of the maturity of the specimen designed by Richard, we uses CTS specimen in our study (as shown in Figure 3). When the specimen is used for fracture toughness test, the initial crack length a_0 is 50mm, the radius of bolts r is M14, while $a_0=35$ mm, $r=12$ mm in fatigue test. The material is aluminum alloy 2024-T351. In view of changing the hole position, A 1/4 circular loading device is applied to suppose the mode I-II load on specimen. The range of loading angle α is $0^\circ \sim 90^\circ$. The schematic diagram of experimental setup is shown in Figure 4.



a) CTS specimen b) Butterfly-type specimen c) T-type specimen

Figure 2 -The specimens applied on the research of mixed-mode fracture criteria

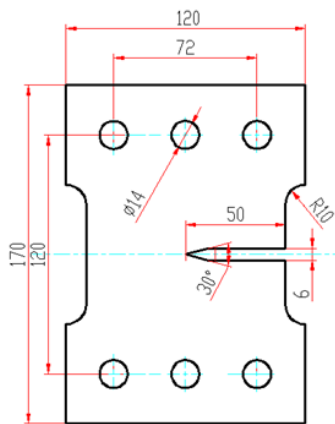


Figure 3 -Geometrical size of CTS specimen



Figure 4 - Experimental setup of CTS specimen under mixed-mode loading

3.2 Static Experimental Results

The specimen was firstly pre-cracked by 2mm with a constant amplitude spectrum load. Then static load was supposed on CTS specimen until unstable crack propagation appears. According to the failure load value, we can obtain the apparent fracture toughness value by FEM.

A total of 17 mixed-mode fracture toughness experiments were carried out on static test pieces, three specimens were selected as a group for the test with different loading angle of 0° , 15° , 30° , 45° , 60° , and two specimens were selected for the experiment with a loading angle of 75° . Figure 5 is the fracture morphology of CTS specimens. Under the tensile and shear mixed-mode loading, the fracture surface is sharp, bright and rough. With the loading angle increased, the deflection angle of fracture surface gradually increases. Table 1 describes the failure load and deflection angle, the results are similar to the results of CTS specimens in Reference [10].

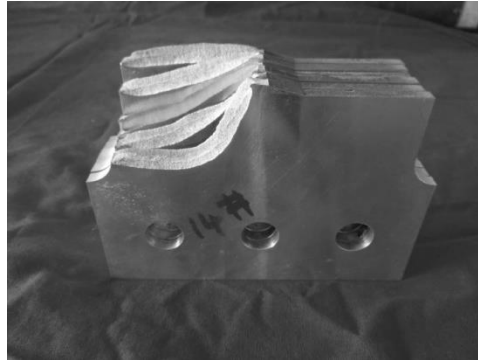


Figure 5 -Failure modes of fracture roughness tests for specimens under different loading angles (0° , 15° , 30° , 45° and 60°)

3.3 Fatigue Experimental Results

The constant fatigue load spectrum at $\alpha=0^\circ$ was first applied on the fatigue tests of CTS structure, and this made the specimens pre-cracked approximately 3mm. Then fatigue load spectrum at 15° , 30° and 45° were supposed on the specimen until it fails. The details of fatigue load are described in Table 2.

Table 2 - Mixed-mode loading design of CTS specimens

Loading angle	Maximum load/kN	Stress ratio
0°	8	0.1
15°	8	0.1
30°	8	0.1
45°	9	0.1

A total of 8 specimens were carried out in the fatigue tests. Considering the small dispersion of the experimental results of crack growth, every 2 specimens were used as a group for the fatigue tests at 0° , 15° , 30° , 45° . Table 2 is the experimental results of the crack growth lives and the crack deflection angle. The loading angle has an important role on the propagation life of CTS specimens, and cracks basically propagate in a direction perpendicular to the cyclic load. Figure 3 are the fatigue failure modes of CTS specimens. The fracture surfaces have smooth stripes, and the fatigue crack growth line can be clearly visible, and specimen belongs to fatigue failure.

Table 1 Fracture toughness results of mixed-mode loading tests

Loading angle	Number	Failure load/kN		Cracking deflection angle	
		Individuals	Mean	Individuals	Mean
0°	1	29.3	28.80	0°	0°
	2	28.86		0°	
	3	28.23		0°	
15°	4	29.18	29.27	-14°	-15.2°
	5	29.26		-17.5°	
	6	29.38		-14°	
30°	7	32.40	31.41	-28.5°	-28.5°
	8	30.60		-28°	
	9	31.24		-29°	
45°	10	34.72	33.84	-45°	-44.2°
	11	33.08		-43.5°	
	12	33.73		-44°	
60°	13	38.30	37.91	-57°	-57.3°
	14	37.54		-57°	
	15	37.90		-58°	
75°	16	43.33	44.35	-72°	-71°
	17	45.38		-70°	

Table 3 -Results of crack growth experiments

Num	Pre-cracked length /mm	failure length /mm	loading angle /°	deflection angle/°	lives/ cycles
1#	3.1	70	0	0	131675
2#	3	71		0	123135
3#	3	75.5	15	16	105460
4#	3.1	75.8		17	98942
5#	3	70.6	30	31	113598
6#	3	71.0		30	112978
7#	3	71.1	45	40	90819
8#	3	72.1		41	88084



a) Failure models



b) Characteristics of fatigue fracture appearance

Figure 6 - Failure modes and fracture appearance of CTS specimens under fatigue loading at 0°, 15°, 30°, 45°

4. Finite Element Analysis of CTS Specimens

4.1 Finite Element Model

As shown in Figure 7, finite element model is built based on ABAQUS. Coupling form are applied to simulate the connection among clamped plate, specimen and bolts. Here we simplify bolts as beam elements. The material of clamped plate and bolts are 30CrMnSiA, where $E_1 = 210000MPa$,

$\nu_1 = 0.33$; the material of specimen is aluminum alloy 2024-T3, which $E_2 = 72000\text{MPa}$ and $\nu_2 = 0.33$.

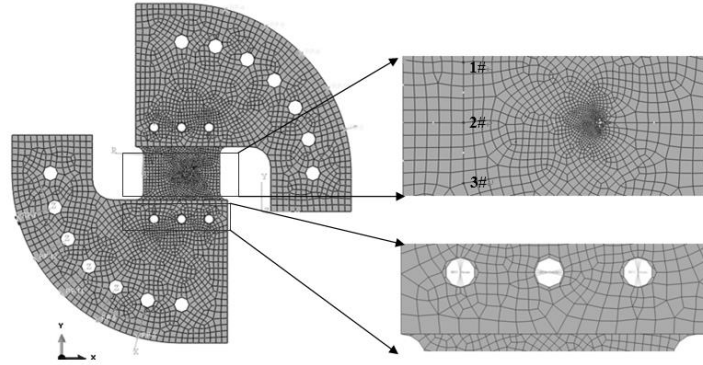


Figure 7 - FE model

For the sake of verifying the feasibility of FE model, we apply this model to analyze the strain distribution of CTS specimens with 35mm crack length supposed on 8000N loading. Table 3 shows the stress value of points 1#, 2# and 3# in Y direction. Points 2# is located in front of the crack tip with 45mm away; Point 1# and point 3# are respectively located directly above and below 2#, and the distance is 20mm away from 2#. We set 3 strain gauges to record the strain changes of these points under a certain load value. The experimental results and FE analysis results show that: the stress values in front of crack tip are similarly uniform, and the maximum error of the stress results between FE and experiments is 4.36%.

Table 4 -Comparisons of σ_y analysis and experimental results on CTS specimen (0° , 8000N)

Num.	Experimental results/ MPa	Simulation results/MPa	Error
1#	11.34	11.26	0.7%
2#	10.66	10.7	0.37%
3#	11.92	11.4	4.36%

4.2 Apparent Fracture Roughness Analysis

The SIF of the specimen under instable load at different loading angle are obtained by applying contour integral technology in the validated finite element model, as shown in Table 5. When the loading angle is equal to 0° , K_{II} can be ignored compared with K_I . Therefore K_I is regarded as the mode-I apparent fracture toughness of CTS specimen. According to the literature [12], For 2024-T351 aluminum alloy with 5mm thickness, the fracture toughness in plane stress state is $3320.00\text{MPa} \cdot \text{mm}^{1/2}$, and the one in plane strain state is $1106.80\text{MPa} \cdot \text{mm}^{1/2}$, and K_{IApp} that we obtained in this paper is consistent with the definition of apparent fracture toughness.

As the loading angle increases, the stress state of the crack is transformed from the mixed tension-shear mode dominated by tensile load to that dominated by shear load. And the instable load for CTS specimens gradually increases. In addition, the crack deflection angle is obtained by MTS criterion in FE model (in Table 5). When the loading angle is larger than 15° , the prediction error increases with the loading angle increased. When loading angel is 75° , error is 15.45%.

Table 5 - SIF analysis of CTS structure under different loading angles

Loading angle	K_I / $\text{MPa} \cdot \text{mm}^{1/2}$	K_{II} / $\text{MPa} \cdot \text{mm}^{1/2}$	Crack deflection angle(MTS principle)	Error
0°	2210.86	0.12	0°	0
15°	2170.8	270.1	13.8°	9.21%
30°	2088.4	560.15	26.8°	5.96%
45°	1836.62	853.565	38.63°	12.60%
60°	1454.09	1171.25	49.6°	13.44%
75°	879.132	1528.3	60.03°	15.45%

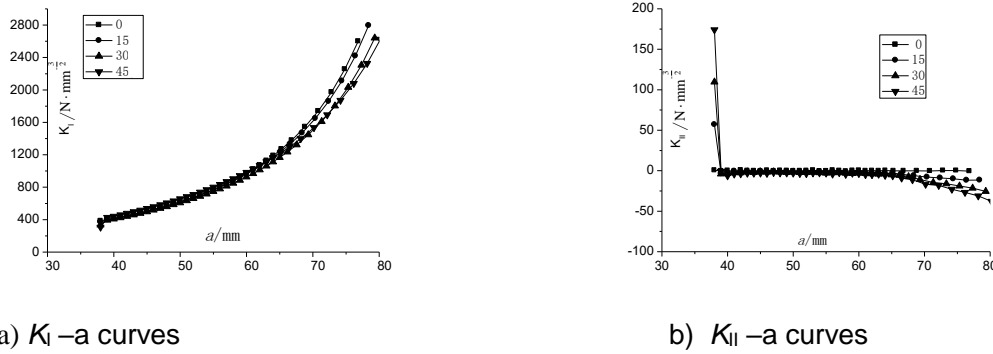
4.3 Evolution of SIF in Mixed-mode Crack Structure

FRACTURE CRITERION ANALYSIS AND CRACK GROWTH PROPERTY OF MIXED-MODE CRACK EXPERIMENTS

Combined with contour integral technology and MTS criterion in ABAQUS, the SIF and crack growth direction can be obtained through parametric modeling by PYTHON, then crack growth length can be calculated by crack growth rate model, the new crack tip is updated according to the growth length. The code will automatically remodel and analyze the crack information until the structures arrived to its residual strength.

Evolution of SIF in Mode-I, Model-II state and crack deflection angle with crack length are shown in Figure 8, Figure 9 and Figure 10. K_I decreases and K_{II} increases with the loading angle increased in the initial crack length state. Once the crack deflected, K_{II} decreases approximated to 0 rapidly. Crack deflection angle is nearly perpendicular to the loading direction and nearly consistent with the direction of principal stress. With the crack length increased, the angle changes are not obvious. When crack length reaches to 60mm, K_{II} begins to increase. The results are considered due to the following reasons:

- The fixtures have some limit to the deflection direction of specimen;
- The T-stress part of circumferential stress at crack tip cannot be ignored when structure is near to the instable state.



a) K_I - a curves

b) K_{II} - a curves

Figure. 8 - Evolution of SIF for CTS specimens under different loading angles

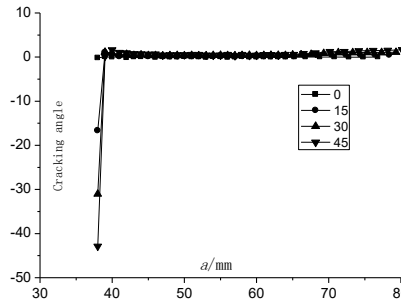


Figure. 9 - Changes of cracking angle with crack length a under different loading angles

5. Numerical Analysis of Mixed-mode Experiments

5.1 Mixed-mode Fracture Toughness

Several fracture criteria based on fracture parameters have been proposed to analyze the fracture mechanism of 2D mixed-mode problem, such as Maximum Circumferential Normal Stress (MTS), minimum Strain Energy Density (SED), Richard criterion based on equivalent Stress Intensity Factor (SIF), Von Mises failure criterion (VMF), and so on. Figure 10 are the comparisons of fracture toughness curves of different failure criteria on CTS specimen. When $\alpha = 0^\circ, 15^\circ$ and 30° , the results obtained by SED, VMF, MTS and Richard criteria are in good agreement with experiments results; When $\alpha > 30^\circ$, MTS and Richard criteria obtained the conservative results compared with the ones by SED and VMF criteria.

Combined with the mode-I/II SIF, we propose a new mode-I/II fracture criterion, which is described as following:

$$K_{II} / K_{IApp} = y_0 + A e^{-\frac{K_I}{K_{IApp}} / t_1} + B e^{-\frac{K_I}{K_{IApp}} / t_2} \quad (19)$$

Where Y_0, A, B, t_1, t_2 are the parameters depending on material and specimen geometry, K_{IApp} is mode-I

apparent fracture toughness. This criterion proposes that unstable fracture occurs when the mode-II SIF reaches the limit value obtained by formula (19). This criterion is derived based on the experimental results of CTS specimen under different loading cases ($0^\circ, 15^\circ, 30^\circ, 45^\circ, 60^\circ$ and 75°). Consequently it basically works for CTS specimens between 0° and 75° .

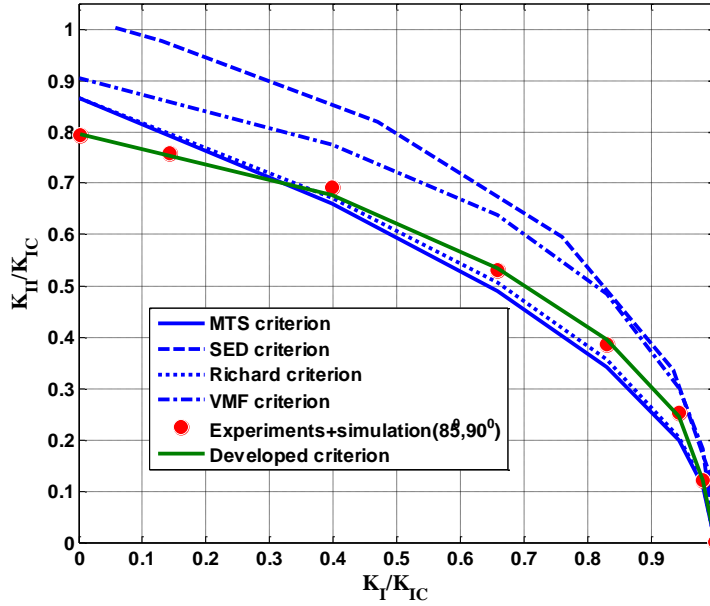


Figure 10- Fracture toughness curves of CTS specimens by different fracture criteria

Similarly, we obtained the failure load of CTS specimens under different loading cases, as shown in figure 11. Richard criterion and MTS criterion are more conservative than those by SED and VMF. Yet Richard criterion is consistent with experimental results. Combined with the verified Finite Element model of mixed mode CTS specimens, we analyze the critical fracture load P_f according to the different criteria. Figure 11 shows the comparisons of P_f between analytical and experimental results. We derive the relation between P and loading angle α as following:

$$P_f = -20.47 \cos(\alpha) + 48.93 \quad (20)$$

The failure load of CTS specimens under pure mode-II loading can be obtained based on formula (19).

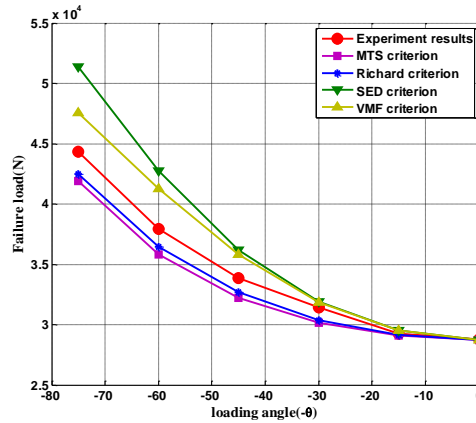


Figure 11 - Relations between loading angle and failure load

When $\alpha = 90^\circ$, K_{II} plays an important role in structural unstable growth. Based on formula (19), $P_f = 48930\text{N}$. Combined with FE analysis, we can get $K_{II} = 1754.94 \text{ MPa} \cdot \text{mm}^{1/2}$, which can be regarded as the mode-II apparent fracture toughness of 2024-T351 aluminum alloy.

5.2 Mixed-mode crack growth model

Fatigue experiments of CTS specimens at different loading cases $15^\circ, 30^\circ$ and 45° were carried out to analyze the life cycles of fatigue crack deflection problem. Crack growth lives based on equivalent SIF by Tanaka formula, simple square root formula, Richard formula and MTS formula are compared with the test results regarding single crack of CTS specimens propagating certain distances. Table 6 is the

comparisons of test results and predictions by formulas (12), (16)~(18) regarding single crack of CTS specimens propagating certain distances. We records the fatigue lives of cracks on CTS specimen at 15°, 30° and 45° loading angle, and obtained that the prediction errors of Formula (18), Formula (17), Formula (12) and Formula (16) are respectively 7.13%, 6.59%, 10.52% and more than 200% compared with experimental results. Table 5 shows that Tanaka formula is more adequate to calculate the equivalent SIF for CTS specimens under mixed-mode I-II loading. Consequently, we apply Tanaka formula in Formula (15) to estimate the fatigue lives of mixed-mode fracture and fatigue problems.

Table 5. Prediction of fatigue lives of CTS specimens at different loading angles

Loading angle	Experimental results	Formula (18)	Formula (17)	Formula (12)	Formula (16)	K _I
15°	31459 (38mm~43.20 mm)	36820	36927	36655	41075	36934
30°	12575 (38mm~39.15 mm)	12316	12780	11556	29177	12954
45°	33203 (38mm~43.22 mm)	32444	32953	30903	311942	34259
Relative error	--	7.13%	6.59%	10.52%	--	7.87%

Figure 12 shows the $da/dN \sim \Delta K_{eq}$ curves of CTS specimens at $\alpha = 0^\circ, 15^\circ, 30^\circ, 45^\circ$. The crack growth rate and the equivalent SIF can be expressed approximately in the form of a power function. Based on the effective SIF described as Formula (17), some authors [12] amended the parameters forms and proposed different fatigue crack growth rate models to evaluate the influences of loading mode on fatigue life. In view of fatigue tests results of CTS specimens on 2024-T3 aluminum, the following crack growth model is proposed:

$$\frac{da}{dN} = ce^{\beta(\frac{2}{\pi} \arctan \frac{K_I}{K_{II}} - 1)} (\Delta K_{eq})^n \quad (21)$$

Where c , n , β are material parameters, and $\beta=1$ when material is 2024-T3 aluminum.

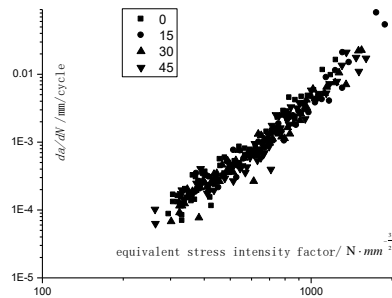


Figure 12 - $da/dN \sim \Delta K_{eq}$ curves under different loading angle ($0^\circ, 15^\circ, 30^\circ$ and 45°)

A rectangular plate with two internal, parallel, non-collinear cracks (length=10mm for both), as shown in Figure 13 is analyzed based on formula (21). A cyclic tension ($\sigma_{max} = 160 \text{ N/mm}$, $\sigma_{min} = 0$) was loaded in a constant spectrum at both ends of plate. The material was chosen as Al 2024-T3 the same as in Reference [13].

The crack propagation path of two non-collinear cracks in $180\text{mm} \times 90\text{mm}$ rectangular plate was analyzed by developed code in Figure 14. Because of the weak interference between two cracks in the initial state, the crack path is straight. With the increase of crack length, the interference effect is clear, the right tip of left crack deflects towards the upper part, as well the left tip of right crack deflects towards the down part, and the elliptical failure mode is formed in the central part. Afterwards, the propagation rate at outside tips of two cracks accelerates, the structure is finally failure. The life of the structure is 6954 cycles, which is in good agreement with the literature [13].

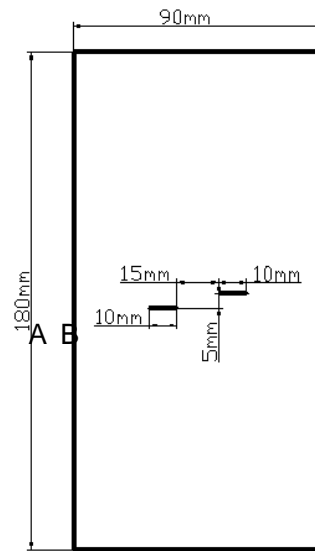


Figure 13 -Plate with two non-collinear cracks

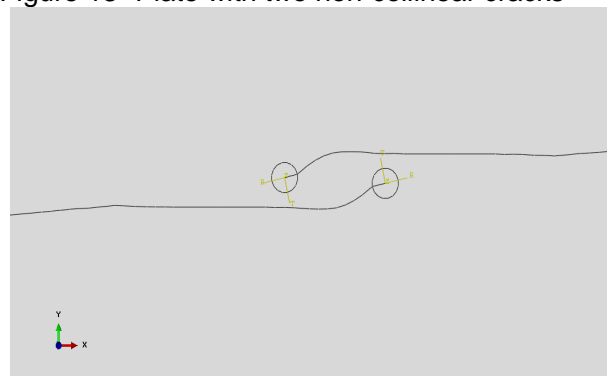


Figure 14 - Crack growth path of plate with two internal collinear cracks

6. Conclusion

The fracture toughness criterion and crack growth behavior of CTS specimens has been investigated both experimentally and numerically. Based on the results analysis, we observe the following points:

- Compared the existing fracture criteria with experimental results in limit load and mixed-mode fracture toughness, mixed-mode fracture toughness based on MTS and Richard criteria are conservative and fitter to engineering analysis. Based on experimental results, we provides some analytical formulas for the calculation of fracture toughness and limit load.
- A new model for mixed-mode crack growth evaluation is proposed based on experimental results, and several forms of equivalent stress intensity factor are analyzed. It is found that the crack of CTS specimen extends vertically along the loading direction, and when the loading angle is in the range of $0^\circ \sim 45^\circ$, Tanaka formula is adequate to calculate the equivalent stress intensity factor for CTS specimens.

7. Contact Author Email Address

mail to: shaopu_su@sina.com

8. Copy right Statement

The authors confirm that they, and/or their company or organization, hold copyright on all of the original material included in this paper. The authors also confirm that they have obtained permission, from the copyright holder of any third party material included in this paper, to publish it as part of their paper. The authors confirm that they give permission, or have obtained permission from the copyright holder of this paper, for the publication and distribution of this paper as part of the ICA proceedings or as individual off-prints from the proceedings.

References

- [1] Erdogan F and G C Sih. On the crack extension in plates under plane loading and transverse shear.

FRACTURE CRITERION ANALYSIS AND CRACK GROWTH PROPERTY OF MIXED-MODE CRACK EXPERIMENTS

Journal of Basic Engineering, No. 85, pp519–525, 1963.

- [2] Sih G C. Strain energy density factor applied to mixed mode crack problems. *International Journal of Fracture*, No. 10, pp305-321,1974.
- [3] Li R, Zhu Z and Xie L. New fracture criterion for mixed mode cracks. *Chinese Journal of Solid Mechanics*. Vol.34, No.1, 2013.
- [4] Richard H A, Schramma B and Schirmeisen N H. Cracks on Mixed Mode loading – Theories, experiments, simulations. *International Journal of Fatigue*. Vol. 62, pp 93-103, 2014.
- [5] YAN X, DU S, ZHANG Z. Mixed mode fatigue crack growth prediction in biaxially stretched sheets. *Engineering Fracture Mechanics*, No. 43, pp 471-475,1992.
- [6] Tanaka K. Fatigue crack propagation from a crack inclined to the cyclic tensile axis. *Engineering Fracture Mechanics*, No. 6, pp 493-507,1974.
- [7] Richard H A. Safety estimation for construction units with cracks under complex loading. *International Journal of Materials & Product Technology*. Vol. 3, pp 326–338,1988.
- [8] Demir O and Ayhan A O. Investigation of mixed mode-I/II fracture problems - Part 2: evaluation and development of mixed mode-I/II fracture criteria. *Fract Struct Integr*, Vol. 35, pp 340–349, 2016.
- [9] Banks-Sills L and Arcan M. An Edge-cracked Mode II fracture specimen. *Experimental Mechanics*, Vol.23, pp 257-261, 1983.
- [10] Husaini and Kikuo K. Investigations of the mixed mode crack growth behavior of an aluminum alloy. *ARPJ Journal of Engineering and Applied Sciences*, Vol.11, No.2, pp.885-890,2016.
- [11] ZHENG X. *Handbook of civil aircraft structural durability and damage tolerance design: fatigue design and analysis*. Beijing: Aviation Industry Press, 2003.
- [12] Ma S and Hu H. The mixed-mode propagation of fatigue crack in CTS specimen. *Chinese Journal of Theoretical and Applied Mechanics*, Vol. 5, No.38, pp.698-704,2016.
- [13] Tu ST and Cai RY. A coupling of boundary elements and singular integral equation for the solution of the fatigue cracked body. *Stress Analysis*, pp 239–247,1993